

# Aggregation kinetics of stiff polyelectrolytes in the presence of multivalent salt

Hossein Fazli

*Institute for Advanced Studies in Basic Sciences, Zanjan 45195-1159, Iran*

Ramin Golestanian\*

*Department of Physics and Astronomy, University of Sheffield, Sheffield S3 7RH, UK*

(Dated: January 11, 2021)

Using molecular dynamics simulations, the kinetics of bundle formation for stiff polyelectrolytes such as actin is studied in the solution of multivalent salt. The dominant kinetic mode of aggregation is found to be the case of one end of one rod meeting others at right angle due to electrostatic interactions. The kinetic pathway to bundle formation involves a hierarchical structure of small clusters forming initially and then feeding into larger clusters, which is reminiscent of the flocculation dynamics of colloids. For the first few cluster sizes, the Smoluchowski formula for the time evolution of the cluster size gives a reasonable account for the results of our simulation without a single fitting parameter. The description using Smoluchowski formula provides evidence for the aggregation time scale to be controlled by diffusion, with no appreciable energy barrier to overcome.

PACS numbers: 87.15.-v,36.20.-r,61.41.+e

## I. INTRODUCTION

Highly charged polyelectrolytes (PEs) are known to attract each other due to electrostatic correlations brought about by multivalent counterions (ions of opposite charge) [1]. A ubiquitous phenomenon arising from these correlations is the formation of collapsed bundles of stiff PEs [2, 3], which is believed to play a significant role in biological processes such as cell scaffolding dynamics [4] and motility [5]. While our current theoretical understanding of the process of PE bundle formation predicts a macroscopic phase separation, i.e. an infinitely large bundle [6], experiments always find finite-sized bundles [2, 3]. To explain this, it has been suggested that the theoretically expected phase separation may be hindered by kinetic barriers [7], steric effects [8], or frustration of the local structure with energy penalty [3, 9]. The phenomenon of bundle formation has also been studied using computer simulation, which indicated a tendency towards a well defined finite size [10, 11]. Recently, an extensive study on the thermodynamic properties of a condensed bundle with multivalent counterions has been carried out, which shows that finite bundles are stable for an intermediate range of electrostatic couplings whereas at strong enough coupling the bundle could be macroscopic [12]. Multivalent counterions can also induce the structural collapse of single semiflexible polyelectrolytes [13] and highly charged polyelectrolyte brushes [14].

We can understand more about this phenomenon by studying the kinetics of the bundle formation. The angle dependent interaction between two rods has been recently studied [15] and it has been shown that the preferred relative orientation of the two rods has a non-trivial connection with whether the overall interaction

is attractive or repulsive. One would then like to know how this complicated angle-dependent interaction affects the fate of the filament bundle in the course of the aggregation kinetics.

Another question could be the dominant kinetic mode of aggregation. A Brownian dynamics simulation using a model short-ranged attraction between two rods has shown that the rods are most likely to meet in a cross configuration, presumably against a barrier as studied in Ref. [7], and then rotate and slide to adjust into a parallel pair [16]. Another pathway with a lower barrier has been suggested in which a rod will slide parallel to an existing bundle [17]. While these descriptions are typically in terms of pairs of rods or an effective interaction of a single filament with an already formed bundle, it is not clear *a priori* that they are feasible in such a highly correlated system. In particular, the orientational dependence of the many-body interaction between highly charged polymers at close proximity is highly complex and can lead to nontrivial effects, such as spontaneous formation of chiral structures [18]. Recently, an experiment has been performed to probe the kinetics of bundle formation by using two different fluorescently labeled actin filaments, which suggests that actin bundles dynamically exchange filaments with the solution [19]. In light of the new experimental insight into the system, it is important to set up a more systematic study of the kinetics of the aggregation, so that the effect of the nontrivial many-body correlations during the course of the aggregation can be better understood.

Here, we study the kinetics of bundle formation in the bulk solution of stiff polyelectrolytes in the presence of multivalent salt using molecular dynamics (MD) simulations. We find that the PEs undergo an aggregation process with doublets, triplets, etc forming and subsequently feeding into larger clusters. We observe that the initial stage of the kinetics leads to formation of PE bundles that have a clear size selection, up to 10-11 filaments for

---

\*Electronic address: r.golestanian@sheffield.ac.uk

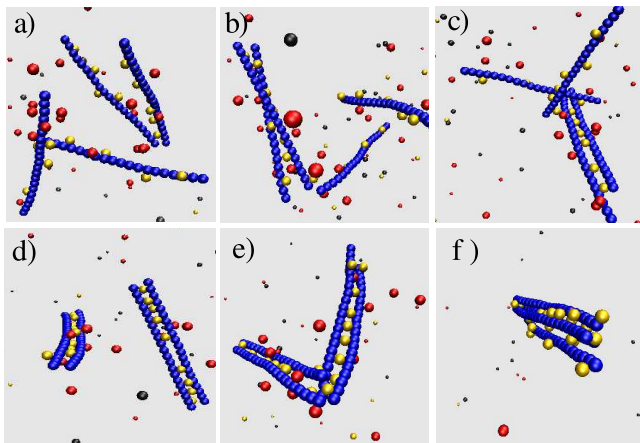


FIG. 1: (color online). Time lapse snapshots of the system with  $N_p = 4$  and  $c_{3:1} = 1$ .  $+3$  salt ions are shown by golden (light) spheres,  $+1$  counterions by red (dark), and  $-1$  salt ions by gray spheres. It can be observed that when two filaments or two bundles meet each other the dominant crossing angle is 90 degrees. In the final configuration all the PEs form a single bundle.

our choice of parameters. These bundles take up all the smaller clusters, and are relatively much more long-lived than the smaller ones, while larger clusters do not seem to appear even when there are a number of these long-lived filament bundles available in the solution for possible aggregation. We find that the time-dependent size distribution of the aggregates follows a Smoluchowski flocculation kinetics. For the first three cluster sizes, namely single filaments, doublets, and triplets, the time evolution of the number of such clusters shows a reasonable quantitative agreement with the Smoluchowski formula when the energy barrier is set to zero. This result shows that the many-body energy barrier for the formation of these clusters is relatively small, and that the time scale for the evolution is set by the diffusion of filaments in the course of the aggregation process. We also monitor the kinetics of bundle growth and find that the dominant mode is due to one end of a filament/bundle meeting another filament/bundle either in the middle mostly at right angle (in the form of “-”) or at one end (in the form of “})”) before rotating and sliding into a parallel packing (see Figs. 1 and 2). We show that these modes can be understood from energetic considerations by calculating the angle dependence of the potential of mean force between two rods.

The rest of the paper is organized as follows. Section II introduces the model and details of the simulation technique used in this work. The main results from the simulation are presented in Sec. III, while Sec. IV is dedicated to the potential of mean force of two rods at various angles and separations. Finally, Sec. V closes the paper with some discussions and remarks.

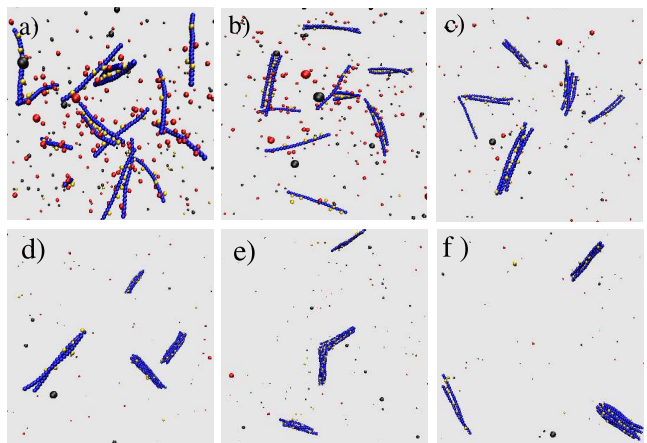


FIG. 2: (color online). Time lapse snapshots of the system with  $N_p = 16$  and  $c_{3:1} = 1$ . The largest bundle contains 11 PE rods (see part f of the figure) and two smaller bundles containing 2 and 3 PEs finally join up and make a bundle of 5 rods (final configuration is not shown in this figure).

## II. THE SIMULATION

In our simulations of the bulk solution, which are performed with the MD simulation package ESPResSo v.1.8 [20],  $N_p$  stiff PEs are considered each composed of  $N_m = 21$  spherical charged monomers of charge  $-e$  (electronic charge) and diameter  $\sigma$  which is introduced via the Lennard-Jones potential (see below). Monomers of each PE are bonded to each other with separation between them being fixed at  $1.1\sigma$  via a finite extensible nonlinear elastic (FENE) potential [21] and the bending rigidity of PE chains is modeled with a bond angle potential  $U_\phi = k_\phi(1 - \cos \phi)$  with  $k_\phi = 400 k_B T$  in which  $\phi$  is the angle between two successive bond vectors along the PE chain. We use  $N_c = N_p \times N_m$  monovalent counterions with charge  $+e$  to neutralize the PEs. We also consider trivalent salt with  $N_s^+$  positive ions with charge  $+3e$  and  $N_s^- = 3N_s^+$  negative ions with charge  $-e$ . In addition to long-ranged Coulomb interaction we include short-ranged Lennard-Jones repulsion between particles, which introduces an energy scale  $\epsilon$  into the system. MD time step in our simulations is  $\tau = 0.01\tau_0$ , in which  $\tau_0 = \sqrt{m\sigma^2/\epsilon}$  is the MD time scale and  $m$  is the mass of the particles.

The temperature is fixed at  $k_B T = 1.2\epsilon$  using a Langevin thermostat. We use the particle-particle particle-mesh (PPPM) method to apply periodic boundary conditions for long-ranged Coulomb interaction in the system. The strength of the electrostatic interaction energy relative to the thermal energy can be quantified using the Bjerrum length  $\ell_B = \frac{e^2}{\epsilon k_B T}$ , where  $\epsilon$  is the dielectric constant of the solvent and in our simulations we have used it to fix the value for  $\sigma$  via  $\ell_B = 3.2\sigma$ . Following Ref. [15], we define the salt concentration as  $c_{3:1} = N_s^-/N_c$ , and use values in the range of  $c_{3:1} = 0.5 - 1.2$ . The Debye length  $\lambda_D = 6\sigma$  for  $c_{3:1} = 1$ .

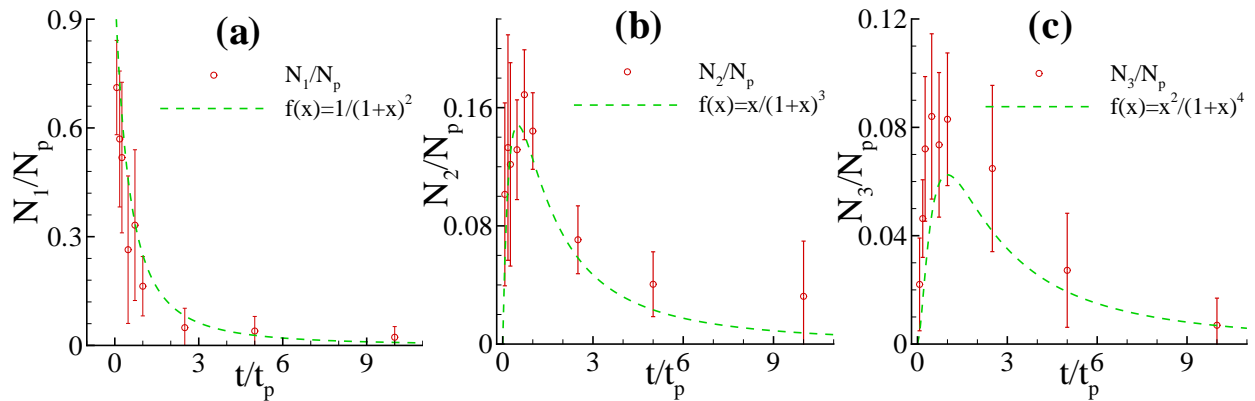


FIG. 3: (color online).  $N_k/N_p$  versus rescaled time  $t/t_p$  for (a)  $k = 1$ , (b)  $k = 2$ , and (c)  $k = 3$ , with  $W = 1$ . Data and error bars are obtained from averaging over sets of data such as those presented in Table I corresponding to various simulations with identical and differing values of  $N_p$ .

In the beginning of the simulations, we fix the PE rods in space parallel to each other with their centers arranged on a square lattice of spacing in the range of  $10\sigma - 15\sigma$  in the middle of the simulation box and all of the ions are free to move for 100,000 MD time steps. We then release the PEs and after equilibration of the system we study the bundle formation kinetics for 8,000,000 MD steps.

### III. RESULTS

We do simulations for different values of the number of PEs ( $N_p = 4, 9, 16, 25, 64$ ) and find that in simulations with 4 and 9 PE rods, in the final configuration of the system a single bundle of parallel PEs forms containing all of them. Figure 1 shows snapshots of the system with  $N_p = 4$  PE rods at different times. It can be seen that PEs that are going to be added to a bundle of parallel PEs, first meet the bundle at right angle and then the crossing angle vanishes.

Simulations with larger  $N_p$  show the same kinetic process (see Fig. 2) as well as an aggregation with small clusters forming initially and then feeding into larger clusters. Table I shows the numbers of PE bundles of different sizes at different times for the simulation with  $N_p = 25$ . In this table,  $N_k$  is the number of bundles containing  $k$  PEs and for a system with  $N_p$  PEs it is subject to the normalization  $\sum_k kN_k = N_p$ . The largest bundle at long times contains 11 PEs in all the simulations. In the case of  $N_p = 16$ , two bundles containing 5 and 11 rods remain at long times with no affinity towards each other when we ran the simulation for longer times. Simulations with larger numbers of PEs, i.e.  $N_p = 25$  (see Table I) and 64 confirm that the growth of the bundles tend to be cut off, or slowed down beyond the time span of our simulation, when there are 10-11 filaments in the bundle. While at the end of the simulation there are more bundles as the number of rods increases, the largest bundle at long times remains to be made of maximum 11 rods.

The evolution of the clusters and their distribution—as exemplified in Table I for 25 rods—resembles the aggregation kinetics of colloidal particles [22]. For the case of spherical colloidal particles with short-ranged interactions, Smoluchowski suggested an (approximate) expression for the number of clusters of size  $k$  in time  $t$  as [22]

$$N_k(t) = \frac{N_p(t/t_p)^{k-1}}{(1+t/t_p)^{k+1}}. \quad (1)$$

In this equation, the characteristic time is defined as

$$t_p = \frac{\eta W}{n_0 k_B T}, \quad (2)$$

where  $\eta$  is the viscosity of water,  $n_0$  is the initial number density of the particles, and  $W \simeq e^{E_a/k_B T}$  is an activa-

TABLE I: Distribution of PE bundle sizes for different values of MD time for a system with  $N_p = 25$  and  $c_{3:1} = 1$ .

time( $\times 2000\tau$ )	$N_1$	$N_2$	$N_3$	$N_4$	$N_5$	$N_6$	$N_{10}$
10	18	2	1	0	0	0	0
35	14	4	1	0	0	0	0
42	13	3	2	0	0	0	0
92	10	3	3	0	0	0	0
144	9	3	2	1	0	0	0
158	8	3	1	2	0	0	0
270	7	2	0	2	0	1	0
350	5	3	0	2	0	1	0
400	4	3	0	1	1	1	0
450	4	3	0	0	1	0	1
750	3	2	1	0	1	0	1
1500	2	2	0	1	1	0	1
2000	2	0	0	2	1	0	1
2700	1	0	0	1	0	0	2
2900	0	0	0	0	1	0	2
4000	0	0	0	0	1	0	2

tion factor (up to a numerical coefficient). The values of  $N_k/N_p$  for  $k = 1, 2$  and  $3$  obtained from our simulations are plotted in Fig. 3 as a function of  $t/t_p$  with  $W = 1$ . In these plots, we have taken  $\eta \simeq 2.4\sqrt{m\epsilon}/\sigma$  (from Ref. [23]),  $k_B T = 1.2\epsilon$ ,  $n_0 = 0.001 \sigma^{-3}$ , and  $\tau = 0.01\tau_0 = 0.01\sqrt{m\sigma^2/\epsilon}$ , which yields  $t_p = 2 \times 10^5 \tau W$ . The results are compared in Fig. 3 with the Smoluchowski formula of Eq. (1) and an agreement in the range of the error bars can be seen. Naturally, the fact that the clusters do not exceed the maximum size of 10-11 means that the analogy is limited to the smaller sizes. Nevertheless, it is remarkable that the same value for  $t_p$  gives a good agreement for  $N_1/N_p$ ,  $N_2/N_p$  and  $N_3/N_p$ , without even a single fitting parameter being used.

The fact that  $W = 1$  seems to provide a reasonable agreement suggests that the PE rods do not experience substantial energy barriers in their “optimal” kinetic paths in the course of the aggregation, although an exact knowledge of the numerical prefactor for  $W$  in the rod geometry is required for a precise determination of the “activation energy”  $E_a$  (which may even turn out to be negative). Note that the low optimal energy barrier does not mean that energetics does not play a role in the kinetics, as the dominant kinetic mode is clearly a result of strong electrostatic interactions.

The problem of quantifying the kinetic barrier of the aggregation process is a complicated one, as it is not clear how one can approach it better than just looking at pair-potentials. Here we propose that monitoring the time evolution of the cluster sizes could be a good alternative for capturing the many-body essence of the aggregation process. The typical time scale  $t_p$  that is involved in the evolution of the cluster sizes [see Eq. (2)] has a diffusion-controlled component  $\eta/(n_0 k_B T) \sim \ell^3/(LD)$ , where  $\ell = n_0^{-1/3}$  is the initial average distance between the filaments in the solution,  $L$  is the length of the filaments, and  $D$  is a filament diffusion coefficient. The second component of  $t_p$  comes from the many-body energetics of the system. A comparison of the simulation results for the cluster sizes with the Smoluchowski formulas in Fig. 3 suggests that the diffusion part is dominant during the early stages of the aggregation until the finite-sized bundles are formed. The fact that the Smoluchowski plots for zero energy barrier are close to the simulation data points, shows that the energy barriers have to be small. We chose to plot the zero energy barrier form instead of trying to fit the data to the Smoluchowski formula and deduce an energy barrier, because we do not know the right prefactors for the different geometry of rods (rather than spheres in the original Smoluchowski solution). However, these prefactors must not differ too much from unity and therefore the argument that the barrier must be small at this stage will be justified from the agreement in Fig. 3.

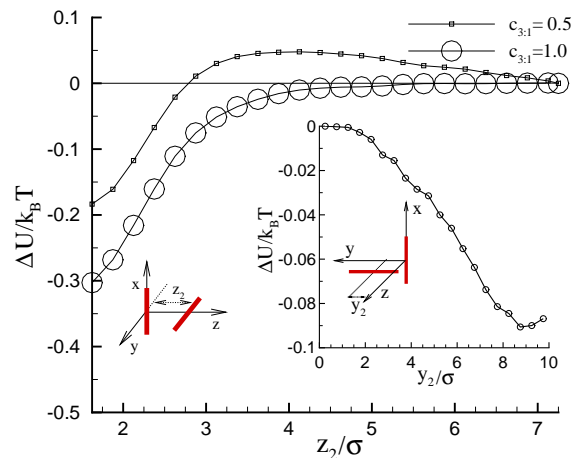


FIG. 4: (color online). Potential of mean force per monomer between two perpendicular rods as a function of the separation between their centers  $z_2$ . The size of the circles on  $c_{3:1} = 1.0$  curve corresponds to the error bars. Inset: potential of mean force between two rods which are perpendicular as a function of  $y_2$  with  $c_{3:1} = 0.7$ .

#### IV. ANGULAR DEPENDENCE OF THE POTENTIAL OF MEAN FORCE

To understand the dominant kinetic mode of PE aggregation we study the different configurations of two rods and keep them fixed during simulation while allowing the counter-ions and salt ions to move freely. In these simulations, we calculate the average force on each monomer and obtain the total force and torque for each PE rod. By integrating the average force (torque) over different separations (orientation angles), we obtain the potential of mean force over a displacement (rotation about an axis) [15]. Let us denote the coordinates of the centers of PEs 1 and 2 as  $(x_1, y_1, z_1)$  and  $(x_2, y_2, z_2)$  respectively (see the schematic configuration of the rods in Fig. 4).

We first show that in the range of salt concentration we use in our simulations, there is an attractive interaction between two PE rods which are perpendicular to each other. Assume that rod 1 is fixed on the  $x$  axis with its center at the origin, and rod 2 is parallel to the  $y$  axis with the coordinates of its center being  $(0, 0, z_2)$ . Figure 4 shows the potential of mean force, which is calculated as the reversible work to bring rod 2 from  $z_2 = 7.5\sigma$  to closer separations as a function of  $z_2$ , for two values of salt concentration  $c_{3:1} = 1$  and  $0.5$ . It can be seen that there is an attractive interaction between two perpendicular PEs. We also calculate the potential of mean force between two perpendicular rods when  $z_2$  is kept fixed at  $z_2 = 1.5\sigma$ , and  $y_2$  is changed (see the schematic configuration in the inset of Fig. 4) for  $c_{3:1} = 0.7$ . We find that the potential of mean force decreases with increasing  $y_2$ , which shows that when the two rods are perpendicular at close separations, the best configuration is when one end of one rod touches the other at right angle (although

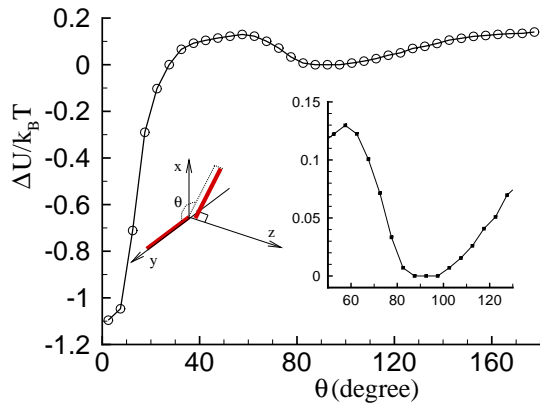


FIG. 5: (color online). The potential of mean force per monomer as a function of  $\theta$  for  $c_{3:1} = 0.7$ . A local minimum can be seen around  $\theta = 90^\circ$ , which is also shown as the inset of the figure. The size of the circles in the main figure shows the error bar.

the potential of mean force is only slightly lower).

We also fix rod 1 on the  $x$  axis with its end at the origin and fix one end of rod 2 at  $(0, 0, 1.5\sigma)$  (see Fig. 5), and calculate the angular dependence of the potential of mean force by integrating the torque with respect to the rotation angle  $\theta$  (around  $z$  axis). In Fig. 5, the orientational dependence of the potential of mean force of the two rods is shown relative to the  $\theta = 90^\circ$  configuration. In this figure, we can see that although the global minimum of the potential of mean force corresponds to parallel configuration of the rods, a local minimum exists around  $\theta = 90^\circ$ , which is shown in detail in the inset of the figure. The attractive interaction between two parallel PEs in the presence of multivalent salt appears only at short separations [15]. This means that for two rods at larger separations, it is more likely that they attract each other when they have larger relative angles, and one of the ends is meeting the other PE in the solution. Moreover, Fig. 5 shows that although the local minimum is shallow compared to the parallel-configuration minimum, it covers a relatively wider range of  $\theta$ , and thus crossing at “nearly” right angle has a considerably high probability. For obtaining each point of Figs. 4 and 5, we have used  $1.5 \times 10^5$  MD steps for equilibration of the system and averaging is done over  $3 \times 10^5$  MD steps.

## V. DISCUSSION

In a recent experiment, the kinetics of bundle formation of actin in the presence of multivalent salt has been monitored, using fluorescence microscopy, and it has been found that the initial stage of bundle growth tends to saturate when the bundles reach the size of 10-20 filaments [19]. The experiment suggests that the bundles at this stage very actively exchange single filaments with the solution, and do not seem to be trapped in a non-

equilibrium state that is hindered by kinetic barriers. It also shows that at later stages the bundles grow longitudinally, while still keeping the same thickness [19]. A similar kinetic pattern is observed in our simulations, showing an initial bundle formation that appears to suddenly “saturate” or drastically slow down in its growth when the size of 10-11 is reached. It should be noted, however, that in our simulation we did not probe the equilibrium structure of the system and therefore our results do not provide conclusive information on the equilibrium distribution of the bundle sizes. We also note that we did not observe the longitudinal growth within our simulation time scale, which is consistent with the experimental observation that the time scale for the diffusion-limited aggregation (DLA) of the already formed bundles is 2-3 orders of magnitude longer than the bundle formation time scale [19]. It is worth mentioning, however, that a Smoluchowski type kinetics does describe even the later stages of the evolution in the experiment which involves time scale of the order of *hours*, but interestingly this rather long time scale is indeed mostly set by the diffusion component of the aggregation time scale  $t_p$  [Eq. (2)] and the actual energy barrier to overcome is quite small (of the order of  $k_B T$ ) [19]. This suggests that our proposed scheme of quantifying the kinetics of the growth within the framework of a flocculation dynamics which takes into account both the availability of the constituents (controlled by diffusion) and the energetic barriers to overcome can help us better understand the problem of finite bundle formation. In other words, just because a part of the process is slow in absolute time scale it does not necessarily mean that a large energy barrier is involved. We would like to point out that this delicate issue has not been recognized in the previous literature of polyelectrolyte bundles.

One may wonder whether the simple model used here can properly account for the physics of charged actin protein filaments in solution. In particular, the diameter of F-actin is one order of magnitude larger than the value we have used for our model stiff polyelectrolytes. Looking at the spatial distribution of the charges on the large protein surface, however, one can note that they are distributed on narrow twisted strips with a helical pitch that is considerably larger than the Debye length. This means that the effective portions of the charge distribution on the actin filaments that interact with each other are in fact not too different from thin short rods of the same charge density. Since the Debye screening length is much smaller than the pitch, one expects that the twist structure does not matter that much at this stage. Another important point is that finite-sized bundle formation has been observed in a variety of bio-polyelectrolytes such as actin, microtubule etc., each of which having very different detailed structures [2]. The generality of the observed phenomenon suggests that the details of the individual systems are probably not the key determining factor in the formation of finite bundles. Since all of the bio-polymers that make finite bundles are highly charged,

one is naturally led to the important question of whether electrostatics alone can cause this effect. This is why observation of a tendency to form finite bundles in simple model polyelectrolytes like ours could provide the key to understanding the physical mechanisms behind this phenomenon.

Finally, we would like to remark on a similar work that has been recently performed by Sayar and Holm, in which the thermodynamic properties of condensed bundles with multivalent counterions is studied [12]. They use a hybrid MC-MD technique, and are primarily concerned with finding the ultimate equilibrium properties of the system, rather than the kinetic pathways of going towards that equilibrium which we probe. In this sense, the two works are complementary as they approach a similar problem from different perspectives and with different tools. The main finding of Ref. [12] is that depending on the parameters the equilibrium state of such stiff polyelectrolytes could be both finite bundles and macroscopic condensation. Their results on potential of mean force can be used to deduce energy barriers, which are in agreement with our kinetic estimates. There are also slight differences in the two systems which might cause differences in their behaviors. For example, in Ref. [12] there are no added salt ions and the system just has enough counterions to neutralize. This means that entropic considerations might hamper full neutralization of

the system and thus create additional barriers (for unneutralized bundles). In our case because we have both salt and counterions, the monovalent ions can partake the entropy and therefore the multivalent counterions can happily reside in the bundle areas, which is perhaps a more faithful modeling of the actual environment of such systems.

In conclusion, we have studied the kinetics of the bundle formation for stiff polyelectrolytes in multivalent salt solutions. The distribution of cluster sizes was found to follow a Smoluchowski dynamics, with no appreciable energy barrier in the optimal kinetic paths, in contrast to previous suggestions [7]. We also found that the dominant kinetic mode of aggregation comes from configurations with one end of a rod meeting the other rods at nearly right angle, and not parallel as proposed in Ref. [17]. These results could hopefully shed some light on the controversial issue of the finite size of actin bundles.

### Acknowledgments

It is our pleasure to acknowledge stimulating discussions with Gerard Wong and assistance from Sarah Mohammadinejad.

- 
- [1] C. Holm, P. Kekicheff, and R. Podgornik, *Electrostatic Effects in Soft Matter and Biophysics* (Kluwer, Dordrecht, 2001); Y. Levin, Rep. Prog. Phys. **65**, 1577 (2002); H. Boroudjerdi, Y.-W. Kim, A. Naji, R.R. Netz, X. Schlagberger, and A. Serr, Phys. Rep. **416**, 129 (2005).
- [2] V.A. Bloomfield, Biopolymers **31**, 1471 (1991); R. Podgornik, D. Rau, and V.A. Parsegian, Biophys. J. **66**, 962 (1994); V.A. Bloomfield, Curr. Opin. Struct. Biol. **6**, 334 (1996); J.X. Tang and P.A. Janmey, J. Biol. Chem. **271**, 8556 (1996); J.X. Tang *et al.*, Biochemistry **36**, 12600 (1997); A.P. Lyubartsev *et al.*, Phys. Rev. Lett. **81**, 5465 (1998); J.C. Butler *et al.*, Phys. Rev. Lett. **91**, 028301 (2003); D.J. Needleman *et al.*, Proc. Natl. Acad. Sci. USA **101**, 16099 (2004).
- [3] T.E. Angelini *et al.*, Proc. Natl. Acad. Sci. USA **100**, 8634 (2003).
- [4] T.D. Pollard and J.A. Cooper, Annu. Rev. Biochem. **55**, 987 (1986); P.A. Jamney *et al.*, Nature (London) **345**, 89 (1990); G. Isenberg, Semin. Cell Div. Biol. **7**, 707 (1996); I. Borukhov *et al.*, Proc. Natl. Acad. Sci. USA **102** 3673 (2005).
- [5] M. Karakozova *et al.*, Science **313**, 192 (2006).
- [6] B.-Y. Ha and A.J. Liu, Phys. Rev. Lett. **81**, 1011 (1998); B.I. Shklovskii, Phys. Rev. Lett. **82**, 3268 (1999); C.-I. Huang and M. Olvera de la Cruz, Macromolecules **35**, 976 (2002).
- [7] B.-Y. Ha and A.J. Liu, Europhys. Lett. **46**, 624 (1999).
- [8] M.L. Henle and P.A. Pincus, Phys. Rev. E **71**, 060801(R) (2005).
- [9] G.M. Grason and R.F. Bruinsma, Phys. Rev. Lett., in press (2007).
- [10] M. Stevens, Phys. Rev. Lett. **82**, 101 (1999).
- [11] H.J. Limbach, M. Sayar, and C. Holm, J. Phys.: Condens. Matter **16**, S2135 (2004).
- [12] M. Sayar and C. Holm, Europhys. Lett. **77**, 16001 (2007).
- [13] K. Besteman, S. Hage, N.H. Dekker, and S.G. Lemay, Phys. Rev. Lett. **98**, 058103 (2007); R. Golestanian, M. Kardar, and T.B. Liverpool, Phys. Rev. Lett. **82**, 4456 (1999); R. Golestanian and T.B. Liverpool, Phys. Rev. E **66**, 051802 (2002).
- [14] H. Fazli, R. Golestanian, P.L. Hansen, and M.R. Kolahchi, Europhys. Lett. **73**, 429 (2006).
- [15] K.C. Lee, I. Borukhov, W.M. Gelbert, A.J. Liu, and M.J. Stevens, Phys. Rev. Lett. **93**, 128101 (2004).
- [16] X. Yu and A.E. Carlsson, Biophys. J. **87**, 3679 (2004).
- [17] T.T. Nguyen and B.I. Shklovskii, Phys. Rev. E **65**, 031409 (2002).
- [18] H. Fazli, R. Golestanian, and M.R. Kolahchi, Phys. Rev. E **72**, 011805 (2005).
- [19] G.H. Lai, O.V. Zribi, R. Coridan, R. Golestanian, and G.C.L. Wong, Phys. Rev. Lett. **98**, 187802 (2007).
- [20] H.J. Limbach, A. Arnold, B.A. Mann and C. Holm, Comp. Phys. Communications, **174**, 704 (2006).
- [21] G.S. Grest and K. Kremer, Phys. Rev. A **33**, 3628 (1986).
- [22] W.B. Russel, D.A. Saville, and W.R. Schowalter, *Colloidal Dispersions* (Cambridge University Press, Cambridge, U.K., 1988).
- [23] B. Dünweg and K. Kremer, Phys. Rev. Lett **66**, 2996 (1991).